Journal of Physical Sciences, Vol. 15, 2011, 43-57
ISSN: 0972-8791, www.vidyasagar.ac.in/journal
Published on 22 December 2011

Micropolar Fluid Flow Through a Channel - *A Mathematical Model for Lung Alveolar Sheet*

Sushil Kumar Ghosh

Department of Mathematics, Garhbeta College,
Garhbeta, Paschim Medinipur-721127, India
E-Mail: sushilkumar_ghosh@yahoo.com

Received November 29, 2010; accepted May 8, 2011

ABSTRACT

In this paper, a mathematical model for the flow of micropolar fluid through a channel covered by a porous media has been derived. In the channel space we have assumed the creeping flow. In the porous space the flow is governed by Brinkman's model. Fourier series expansions have been employed to derive the solution of the partial differential equations. The presented analytical results of velocities, pressures and wall shear stress are computed with the desired experimental data, obtained from various important studies and presented graphically with the view of importance in the present context. Investigation shows that the fluid parameters (rotational) are highly significant for the flow in the interstitial space. Apart from this, the effects of some constants (first derived by Tang and Fung [6]) on the interstitial flow are incorporated into the discussion.

Keywords: Micropolar Fluid, porous media, Fourier series, Pulmon-ary circulation, Blood flow, Brinkman's Model.

1. Introduction

Nearly three decades back a number of authors (Eringen and Suhubi, 1964) extended the classical continuum theories by the introduction of higher order kinematics variables. Among these the simplest model allows the material particle to rotate independently of the classical rotation. Tozeren and Skalak(1977) considered the case of suspensions of rigid particles in an incompressible Newtonian fluids with the assumption that there is no systemic translational motion of particle through the ambient fluid. The most frequently cited model that has been adopted in this work is Eringen (1966). One of the suggested useses of micropolar theory (Grzegorz, 1999) is the analysis of blood flow through small arteries. To determine the shear stress at the wall Lee and Fung (1970) numerically analyzed the flow through a locally constricted tube. Tang and Fung (1975) investigated the fluid movement in a channel

with permeable wall covered by a porous media. The motivation was to study the mass transfer in the lung. In subsequent studies (1975, 1975) they presented the solute distribution in the channel space as well as porous space.

All these studies are confined to the problems treating blood as a homogeneous, Newtonian, viscous fluid. Inadequacy of interpretation of blood flow phenomena, several constitutive relations come in to the picture to study the blood flow properly. Owing to a handful experimental observations a model developed mathematically can be verified easily. However, Ariman et. al.(1974) studied the steady and pulsatile blood flow through small rigid circular tube. They served that the microcontinuum theory can interpret blood flow in more appropriate form because it includes the microrotation in the governing equation. This investigation was supported and confirmed by Ariman et al. (1974). About the suitability of micropolar theory Hogan et al. (1989) have presented a wide range of discussions. They quantify the potential differences between classical and micropolar theory for various vessels sizes. The result shows that the wall shear stress differs substantially in the micropolar theory from those obtained with a classical Newtonian fluid. Misra and Ghosh (1997) put forward a mathematical model of the channel flow where the suspended particles have a micro-rotation. Results show that the rotation enhances the fluid transfer into the porous space. In another paper, they also found a significant result when micro-polar fluid passes through a constriction of an artery (2001). It is common to assume that blood vessels are nearly circular cylindrical tube but in the lung, structure differs significantly. The pulmonary circulation in the microvessel is confined between two walls. This may be represented as a sheet like flow. The upper and lower sheets are porous and inner walls are permeable and outer walls are impermeable. The two sidewalls are non-porous and inner wall impermeable. In this case, both the flows in through porous space as well as in the channel space are two-dimensional.

We propose to present here the analysis of a mathematical model for the flow of micropolar fluid through a lung alveolar sheet. Each sheet made of porous material conducts a fluid movement, which is governed by Brinkman's equations. The convective and diffusive terms are neglected in comparison to the resistance term. Thus the local acceleration and resistance to the flow due to the fibrous material in the porous medium balances the pressure gradient. In the channel space, we solved the couple equation with the assumption that the convective terms are negligibly small. Matching boundary conditions are used to couple both the flows. Mass transfer between two regions is performed by the Starling hypothesis. An extensively used Fourier series expansion has been employed to solve the governing equation in both the regions.

2. Mathematical Model:

Figure 1 is the geometry of the system with a two-dimensional coordinates system. Blood is flowing through a channel with variable cross-section. It is considered that the channel diverges exponentially according to the relation

$$h(x^*) = h_0^*(1+\sin \omega t) \tag{1}$$

where ε is the diverging parameter, h, the characteristic thickness, $h^*(t^*)$ the height of the channel. Blood is treated here as a non-Newtonian micro-polar fluid and fluid flowing in the interstitial space is Newtonian. Our aim is to evaluate flow velocity in these two regions along with the pressure distribution. Moreover, a brief study of various parameters will also be performed with due care to validate this model. This work is mainly an extension of Misra and Ghosh (1997).

2.1 Flow in the porous Space: The governing equation for the flow of interstitial space can be represented as

$$\rho\frac{\partial u_{11}^*}{\partial t^*}+\frac{\partial p_1^*}{\partial z^*}=T\mu\left(\frac{\partial^2 u_{11}^*}{\partial x^{*2}}+\frac{\partial^2 u_{11}^*}{\partial z^{*2}}\right)-\frac{\mu}{\kappa}u_{11}^* \tag{2}$$

$$\rho\frac{\partial u_{12}^*}{\partial t^*}+\frac{\partial p_1^*}{\partial z^*}=T\mu\left(\frac{\partial^2 u_{12}^*}{\partial x^{*2}}+\frac{\partial^2 u_{12}^*}{\partial z^{*2}}\right)-\frac{\mu}{\kappa}u_{12}^* \tag{3}$$

$$\frac{\partial u_{11}^*}{\partial x^*}+\frac{\partial u_{12}^*}{\partial z^*}=0 \tag{4}$$

The boundary conditions are

$$u_{11}^*=0, \quad \text{at} \quad x^*=0,\ \text{L}, \tag{5}$$

$$u_{12}^*=0, \quad \text{at;} \quad z^*=\pm(h^*+\delta^*) \tag{6}$$

$$u_{12}^*=\frac{K}{\rho}\left[(p_2^*-p_1^*)-\sigma_1(\pi_2-\pi_1)\right], \ \text{at}\ z^*=\pm h^*(t^*); \tag{7}$$

Here * refers to the dimensional variable and u_{11}^* and u_{12}^* are axial and vertical velocity in the interstitial space. L is the length of the arterial segment of the pulmonary circulatory system, p_1^* and p_2^*, the pressure in the channel space and porous space respectively; σ_1 the reflection coefficient of the wall; δ the thickness of the porous space, π_1, π_2 atmospheric pressures in the porous space and channel space respectively. Density of interstitial fluid is ρ; μ the viscosity, K the permeability constant.

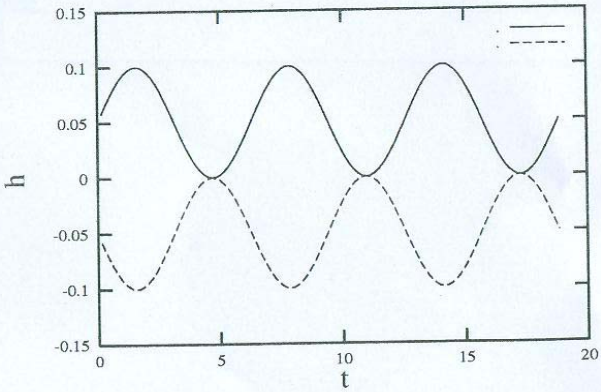

Fig.1 The configuration of the Channel (h_0 =0.05,ω =1.0)

The following non-dimensional variables are introduced in the given governing equations.

$(u_{11}^*, u_{12}^*)/U = (u_{11}, u_{12})$, $(x^*, z^*)/ = (x, z)$, $h^*(t^*)/L = h$, $h_0^*/L = h_0$, $(p_i, \pi_i)\mu U/L = (p_i, \pi_i)$, $\delta^*/L = \delta$, $t^*/\omega = t$, $i = 1,2$, where U is the characteristic velocity of blood. We seek a solution of the following form $\psi_1(x,z,t) = \psi_1(x,z)e^{it}$ Where ψ_1, the stream function and defined as

$$u_{11} = -\frac{\partial \psi_1}{\partial z}, \quad u_{12} = \frac{\partial \psi_1}{\partial x}$$

The dimensionless equations are given by

$$i\alpha^2 \frac{L^2}{h^2}\nabla^2\psi_1 = T\nabla^4\psi_1 - \frac{\rho L^2}{\kappa\mu}\nabla^2\psi_1 \tag{8}$$

where $\alpha^2 = \dfrac{\omega\rho h^2}{\mu}$, $\nabla^2 = \dfrac{\partial^2}{\partial x^2} + \dfrac{\partial^2}{\partial z^2}$

The non-dimensional boundary conditions are

$u_{11} = 0$, at x=0, L, (9)

$u_{12} = 0$, at; $z = \pm(h+\delta)$ (10)

$$u_{12} = \frac{K}{\rho}\left[(p_2 - p_1) - \sigma_1(\pi_2 - \pi_1)\right], \text{ at } \quad z = \pm h(t); \tag{11}$$

The condition (9) leads to the solution of the form $\psi_1(x,z) = f(z)\sin(\lambda_n x)$, where $\lambda_n = n\pi$, $n = 0,\pm1,\pm2,\pm3,\pm4,.....$

(12)

Hence the solution can be written as

$$\psi_1(x,z) = A_n e^{(\lambda_{n1}+i\lambda_{n2})z} + B_n e^{-(\lambda_{n1}+i\lambda_{n2})z} + C_n e^{\lambda_n z} + D_n e^{-\lambda_n z})\sin\lambda_n x \tag{13}$$

$$\begin{aligned} p_1 = &\left[A_n\left\{T(\lambda_{n1}+i\lambda_{n2})\{(\lambda_{n1}+i\lambda_{n2})^2+\frac{1}{\lambda_n}\}-(i\frac{\alpha^2L^2}{h^2}+\frac{\rho L^2}{\kappa\mu})\frac{\lambda_{n1}+i\lambda_{n2}}{\lambda_n}\right\}e^{(\lambda_{n1}+i\lambda_{n2})z}\right]\cos\lambda_n x \\ &+\left[B_n\left\{T(\lambda_{n1}+i\lambda_{n2})\{(\lambda_{n1}+i\lambda_{n2})^2-\frac{1}{\lambda_n}\}+(i\frac{\alpha^2L^2}{h^2}+\frac{\rho L^2}{\kappa\mu})\frac{\lambda_{n1}+i\lambda_{n2}}{\lambda_n}\right\}e^{-(\lambda_{n1}+i\lambda_{n2})z}\right]\cos\lambda_n x \\ &+\left[C_n\left\{2T\lambda_n^2-(i\frac{\alpha^2L^2}{h^2}+\frac{\rho L^2}{\kappa\mu})\right\}e^{\lambda_n z}\right]\cos\lambda_n x + \\ &\left[D_n\left\{-2T\lambda_n^2+(i\frac{\alpha^2L^2}{h^2}+\frac{\rho L^2}{\kappa\mu})\right\}e^{\lambda_n z}\right]\cos\lambda_n x \\ &+P_1(z) \end{aligned} \tag{14}$$

2.2 Flow in the Channel Space:

As the pulmonary alveoli prevails the low Reynolds number flow, the governing equation for the flow of blood can be written in the following form by neglecting the convective terms.

$$\mu\nabla^{*2}u_{21}^* - 2\mu_R\frac{\partial\sigma^*}{\partial z^*} - \frac{\partial p^*}{\partial x^*} = \rho\frac{\partial u_{21}^*}{\partial t^*} \tag{15}$$

$$\mu\nabla^{*2}u_{22}^* - 2\mu_R\frac{\partial\sigma^*}{\partial x^*} - \frac{\partial p^*}{\partial z^*} = \rho\frac{\partial u_{22}^*}{\partial t^*} \tag{16}$$

$$\gamma\nabla^{*2}\sigma^* + 2\mu_R\left(\frac{\partial u_{21}^*}{\partial z^*} - \frac{\partial u_{22}^*}{\partial x^*}\right) - 4\mu_S\sigma^* = \rho j\frac{\partial\sigma^*}{\partial t^*} \tag{17}$$

while the equation of continuity is $\frac{\partial u_{21}^*}{\partial x^*} + \frac{\partial u_{22}^*}{\partial z^*} = 0$, where μ_R, the rotational viscosity, u_{21}^*, u_{22}^* are axial and vertical velocities respectively. γ the microrotational gradient coefficient, j the gyrational parameter, σ^* the rotational velocity along y direction of the particle.

With the earlier non-dimensional scheme we introduce $\frac{\sigma^*}{U}L$ for σ^* and seek a solution $\psi_2^*(x^*,z^*,t^*)=\psi_2^*(x^*,z^*)e^{i\omega t^*}$ and $\sigma^*(x^*,z^*,t^*)=\sigma^*(x^*,z^*)e^{i\omega t^*}$ where ω is the perturbation frequency and ψ_2^* is the stream function in the channel space.

$u_{21}=-\frac{\partial\psi_2}{\partial z}$, $u_{22}=\frac{\partial\psi_2}{\partial x}$, After eliminating p_2, we obtain the dimensionless form in ψ_2 as

$$\nabla^4\psi_2-2\frac{\mu_R}{\mu_S}\nabla^2\sigma=i\alpha^2\frac{L^2}{h^2}\nabla^2\psi_2$$

(18)

$$\nabla^2\sigma-2\frac{\mu_R L^2}{\gamma}\nabla^2\psi_2-\left[\frac{4\mu_S L^2}{\gamma}+\frac{\rho j\omega L^2 i}{\gamma\mu_R}\right]\sigma=0 \tag{19}$$

From (18) and (19) we get

$$\left[\nabla^4+M_P\nabla^2+N_P\right]\nabla^2\psi_2=0 \tag{20}$$

Where $M_P=-\left\{\frac{4\mu_R L^2}{\mu_S\gamma}(\mu_R+\mu_S)+i\frac{L^2\alpha^2}{h^2}(\frac{j\mu_S}{\gamma}-1)\right\}$

$$N_P=-\left\{\frac{jL^4\mu_S\alpha^4}{h^4\gamma}-\frac{4L^4\alpha^4\mu_R}{\gamma h^2}\right\}$$

The boundary and initial conditions in dimensional form are

$u_{21}=0$ at x=0,1 (21)

$u_{21}=0,$ at z=$\pm h$ (22)

$u_{21}=u_{22}$ at $z=\pm h$ (23)

$\frac{\partial u_{21}}{\partial z}=0$ at z=0 (24)

$u_{22}=0$ at z=0 (25)

$\sigma=S\left(\frac{\partial u_{22}}{\partial x}-\frac{\partial u_{21}}{\partial z}\right)$ at $z=\pm h$ (26)

The (21) predicts that the solution can be obtained by eigenfunction expansion method.

We assume that $\psi_2(x,z)=g(z)\sin(\lambda_n x)$ where $\lambda_n=n\pi$,
n= 0,±1,±2,±3,±4,.....

$$\psi_2(x,z) = \{E_n e^{(\lambda_{n3}+i\lambda_{n4})z} + F_n e^{-(\lambda_{n3}+i\lambda_{n4})z} + G_n e^{(\lambda_{n5}+i\lambda_{n6})z} + H_n e^{-(\lambda_{n5}+i\lambda_{n6})z} + P_n e^{\lambda_n z} + Q_n e^{\lambda_n z}\} \sin\lambda_n x \tag{27}$$

$$p_2(x,z) = E_n \left[\frac{(\lambda_{n3}+i\lambda_{n4})\left\{(\lambda_{n3}+i\lambda_{n4})^2 - \lambda_n\right\}+}{\frac{4\mu_R^2 L^2}{\mu_s \gamma}\frac{(\lambda_{n3}+i\lambda_{n4})\{(\lambda_{n3}+i\lambda_{n4})^2 - \lambda_n^2\}}{(\lambda_{n3}+i\lambda_{n4})^2 - (\lambda_{n7}+i\lambda_{n8})^2} - \frac{i\alpha^2 L^2}{h^2}(\lambda_{n3}+i\lambda_{n4})} \right]$$

$$\cdot \frac{1}{\lambda_n} e^{(\lambda_{n3}+i\lambda_{n4})z} \cos\lambda_n x$$

$$+ F_n \left[\frac{(\lambda_{n3}+i\lambda_{n4})\left\{(\lambda_{n3}+i\lambda_{n4})^2 - \lambda_n\right\}-}{\frac{4\mu_R^2 L^2}{\mu_s \gamma}\frac{(\lambda_{n3}+i\lambda_{n4})\{(\lambda_{n3}+i\lambda_{n4})^2 - \lambda_n^2\}}{(\lambda_{n3}+i\lambda_{n4})^2 - (\lambda_{n7}+i\lambda_{n8})^2} + \frac{i\alpha^2 L^2}{h^2}(\lambda_{n3}+i\lambda_{n4})} \right] \frac{1}{\lambda_n} e^{-(\lambda_{n3}+i\lambda_{n4})z} \cos\lambda_n x$$

$$+ G_n \left[\frac{(\lambda_{n5}+i\lambda_{n6})\left\{(\lambda_{n5}+i\lambda_{n6})^2 - \lambda_n\right\}+}{\frac{4\mu_R^2 L^2}{\mu_s \gamma}\frac{(\lambda_{n5}+i\lambda_{n6})\{(\lambda_{n5}+i\lambda_{n6})^2 - \lambda_n^2\}}{(\lambda_{n5}+i\lambda_{n6})^2 - (\lambda_{n7}+i\lambda_{n8})^2} - \frac{i\alpha^2 L^2}{h^2}(\lambda_{n5}+i\lambda_{n6})} \right] \frac{1}{\lambda_n} e^{(\lambda_{n5}+i\lambda_{n6})z} \cos\lambda_n x$$

$$+ H_n \left[\frac{(\lambda_{n5}+i\lambda_{n6})\left\{(\lambda_{n5}+i\lambda_{n6})^2 - \lambda_n\right\}-}{\frac{4\mu_R^2 L^2}{\mu_s \gamma}\frac{(\lambda_{n5}+i\lambda_{n6})\{(\lambda_{n5}+i\lambda_{n6})^2 - \lambda_n^2\}}{(\lambda_{n5}+i\lambda_{n6})^2 - (\lambda_{n7}+i\lambda_{n8})^2} + \frac{i\alpha^2 L^2}{h^2}(\lambda_{n5}+i\lambda_{n6})} \right] \frac{1}{\lambda_n} e^{-(\lambda_{n5}+i\lambda_{n6})z} \cos\lambda_n x$$

$$+ P_n \left[-\frac{4\mu_R^2 L^2}{\mu_s \gamma}\frac{\lambda_n^3}{\lambda_n^2 - (\lambda_{n7}+i\lambda_{n8})^2} - \frac{i\alpha^2 L^2}{h^2}\lambda_n \right] \frac{1}{\lambda_n} e^{\lambda_n z} \cos\lambda_n x$$

$$+ Q_n \left[\frac{4\mu_R^2 L^2}{\mu_s \gamma}\frac{\lambda_n^3}{\lambda_n^2 - (\lambda_{n7}+i\lambda_{n8})^2} + \frac{i\alpha^2 L^2}{h^2}\lambda_n \right] \frac{1}{\lambda_n} e^{-\lambda_n z} \cos\lambda_n x$$

$$+ \frac{2\mu_R}{\mu_s}\frac{S_{n1}}{\lambda_n^2}(\lambda_{n7}+i\lambda_{n8}) e^{(\lambda_{n7}+i\lambda_{n8})z} \cos\lambda_n x +$$

$$\frac{2\mu_R}{\mu_s}\frac{S_{n2}}{\lambda_n^2}(\lambda_{n7}+i\lambda_{n8}) e^{-(\lambda_{n7}+i\lambda_{n8})z} \cos\lambda_n x \qquad + P_2(z) \tag{28}$$

where $\lambda_{n3} = \frac{1}{\sqrt{2}}\sqrt{H_1 + \sqrt{H_1^2 + H_2^2}}$,

$$\lambda_{n4} = \frac{1}{\sqrt{2}}\sqrt{-H_1 + \sqrt{H_1^2 + H_2^2}}$$

$$\lambda_{n5} = \frac{1}{\sqrt{2}}\sqrt{H_3 + \sqrt{H_3^2 + H_4^2}} \qquad \lambda_{n6} = \frac{1}{\sqrt{2}}\sqrt{-H_3 + \sqrt{H_3^2 + H_4^2}}$$

$$H_1 = \frac{G_1 - M_1}{2}, \qquad H_2 = \frac{G_2 - M_2}{2}, \qquad H_3 = -\frac{G_1 + M_1}{2},$$

$$H_4 = \frac{G_2 + M_2}{2},$$

$$G_1 = \frac{1}{\sqrt{2}}\sqrt{z_1 + \sqrt{z_1^2 + z_2^2}} \qquad G_2 = \frac{1}{\sqrt{2}}\sqrt{-z_1 + \sqrt{z_1^2 + z_2^2}}$$

$$z_1 = M_1^2 - M_2^2 - 4N_1, \;\; M_1 = -\left[\frac{4L^2\mu_R}{\gamma} + \frac{4L^2\mu_R}{\gamma\mu} + 2\lambda_n^2 \dot{:}\right],$$

$$M_2 = -\left[\frac{j\alpha^2 L^2 \mu_S}{\gamma h^2} + \frac{\alpha^2 L^2}{h^2}\right],$$

$$N_1 = \left[\frac{L^4\alpha^4\mu_S j}{\gamma h^4} + \lambda_n^4 - \lambda_n^2\left(\frac{4L^2\mu_R^2}{\mu\gamma} - \frac{4L^2\mu_R^2}{\gamma}\right)\right],$$

$$N_2 = \left[\frac{2}{\gamma h^4} L^4\alpha^2\mu_R + \lambda_n^2\left(\frac{j\mu}{\gamma} - 1\right)\frac{\alpha^2 L^2}{h^2}\right]$$

From (19) with the help of (27) we can find

$$\sigma = \sin(\lambda_n x)\left[e^{\lambda_{n7} z}\left(S_1 e^{(\lambda_{n7} + i\lambda_{n8})z} + S_2 e^{-(\lambda_{n7} + i\lambda_{n8})z}\right) + E_n \frac{2L^2\mu_R}{\gamma} e^{(\lambda_{n3} + i\lambda_{n4})z} \frac{(\lambda_{n3} + i\lambda_{n4})^2 - \lambda_n^2}{(\lambda_{n3} + i\lambda_{n4})^2 - (\lambda_{n7} + i\lambda_{n8})^2}\right]$$

$$+ \sin(\lambda_n x)\left[F_n \frac{2L^2\mu_R}{\gamma} e^{-(\lambda_{n3} + i\lambda_{n4})z} \frac{(\lambda_{n3} + i\lambda_{n4})^2 - \lambda_n^2}{(\lambda_{n3} + i\lambda_{n4})^2 - (\lambda_{n7} + i\lambda_{n8})^2}\right]$$

$$+ \sin(\lambda_n x)\left[G_n \frac{2L^2\mu_R}{\gamma} e^{(\lambda_{n5} + i\lambda_{n6})z} \frac{(\lambda_{n5} + i\lambda_{n6})^2 - \lambda_n^2}{(\lambda_{n5} + i\lambda_{n6})^2 - (\lambda_{n7} + i\lambda_{n8})^2}\right]$$

$$+ \sin(\lambda_n x)\left[H_n \frac{2L^2\mu_R}{\gamma} e^{(\lambda_{n5} + i\lambda_{n6})z} \frac{(\lambda_{n5} + i\lambda_{n6})^2 - \lambda_n^2}{(\lambda_{n5} + i\lambda_{n6})^2 - (\lambda_{n7} + i\lambda_{n8})^2}\right]$$

$$+ \sin(\lambda_n x)\left[P_n e^{\lambda_n z} \frac{\lambda_n^2}{\lambda_n^2 - (\lambda_{n7} + i\lambda_{n8})^2}\right] + \sin(\lambda_n x)\left[Q_n e^{-\lambda_n z} \frac{\lambda_n^2}{\lambda_n^2 - (\lambda_{n7} + i\lambda_{n8})^2}\right] \tag{29}$$

where $\lambda_{n7} \pm \lambda_{n8} = \pm\sqrt{S_K + \lambda_n^2}$, $S_K = \frac{4}{\gamma} L^2\mu_R + \frac{\rho j\alpha}{\gamma} i$

2.3 The Wall Shear Stress:

$$\tau_{ij} = -p\delta_{ij} + (2\mu_S + \mu_R)E_{ij} + \mu_S e_{ijk}(\omega_k - \sigma_k)$$

$$\tau_{xz} = (2\mu_R + \mu_S)\frac{1}{2}(U_{x,z} + U_{z,x}) + \mu_S(\omega_k - \sigma_k)$$

$$\tau_{xx} = -p + (2\mu_R + \mu_S)u_{x,x}),$$

$$\tau_{zz} = -p + (2\mu_R + \mu_S)u_{z,z},\ \tau_{zz} - \tau_{xx} = -p + (2\mu_R + \mu_S)(u_{22,z} - u_{21,x}),$$

$$\tau_{xz} = (2\mu_R + \mu_S)\frac{1}{2}(u_{x,z} + u_{z,x}) + \mu_S(\omega_y - \sigma_y), \text{ where, } \omega_y = \frac{\partial u_{21}}{\partial z} - \frac{\partial u_{22}}{\partial x}$$

The wall shear stress at the wall $z = h(t)$ is

$$T = \frac{\tau_{xz}(1 - \frac{da}{dx})^2 + (\tau_{zz} - \tau_{xx})\frac{da}{dx}}{\left\{1 + \left(\frac{da}{dx}\right)^2\right\}} \tag{30}$$

$$\tau_{xz} = \frac{2\mu_R + \mu_S}{2}\left[\frac{\partial u_{21}}{\partial z} + \frac{\partial u_{22}}{\partial x}\right] + \mu_S\left[\frac{\partial u_{21}}{\partial z} - \frac{\partial u_{22}}{\partial x} - \sigma\right], \tag{31}$$

$$\tau_{zz} - \tau_{xx} = (2\mu_R + \mu_S)\left(\frac{\partial u_{22}}{\partial z} - \frac{\partial u_{21}}{\partial x}\right) \tag{32}$$

$$\tau_{zz} - \tau_{xx} = 2(2\mu_R + \mu_s)\begin{bmatrix} E_n(\lambda_{n3} + i\lambda_{n4})\lambda_n e^{(\lambda_{n3}+i\lambda_{n4})h} - F_n(\lambda_{n3} + i\lambda_{n4})e^{-(\lambda_{n3}+i\lambda_{n4})h} \\ + G_n(\lambda_{n5} + i\lambda_{n6})\lambda_n e^{(\lambda_{n5}+i\lambda_{n6})h} - H_n(\lambda_{n5} + i\lambda_{n6})\lambda_n e^{-(\lambda_{n7}+i\lambda_{n8})h} \\ + P_n\lambda_n^2 e^{\lambda_n h} + Q_n\lambda_n^2 e^{\lambda_n h} \end{bmatrix}$$

$$\tau_{xz} = \begin{bmatrix} \frac{2\mu_R + \mu_s}{2}\left\{-(\lambda_{n3} + i\lambda_{n4})^2 - \lambda_n^2\right\} - \\ \mu_s\left\{(\lambda_{n3} + i\lambda_{n4})^2 - \lambda_n^2 + \frac{2\mu_R L^2}{\gamma}\frac{(\lambda_{n3} + i\lambda_{n4})^2 - \lambda_n^2}{(\lambda_{n3} + i\lambda_{n4})^2 - (\lambda_{n7} + i\lambda_{n8})^2}\right\} \end{bmatrix}\{E_n e^{(\lambda_{n3}+i\lambda_{n4})h} + F_n e^{-(\lambda_{n3}+i\lambda_{n4})h}\}\sin\lambda_n x$$

$$+\begin{bmatrix} \frac{2\mu_R + \mu_s}{2}\left\{-(\lambda_{n5} + i\lambda_{n6})^2 - \lambda_n^2\right\} - \\ \mu_s\left\{(\lambda_{n5} + i\lambda_{n6})^2 - \lambda_n^2 + \frac{2\mu_R L^2}{\gamma}\frac{(\lambda_{n5} + i\lambda_{n6})^2 - \lambda_n^2}{(\lambda_{n5} + i\lambda_{n6})^2 - (\lambda_{n7} + i\lambda_{n8})^2}\right\} \end{bmatrix}\{G_n e^{(\lambda_{n5}+i\lambda_{n6})h} + H_n e^{-(\lambda_{n5}+i\lambda_{n6})h}\}\sin\lambda_n x$$

$$-(P_n e^{\lambda_n h} + Q_n e^{-\lambda_n h})\left[\mu_s(2\lambda_n^2 + \frac{\lambda_n^2}{\lambda_n^2 - (\lambda_{n7} + i\lambda_{n8})^2})\right]\sin\lambda_n x$$

All the constants appeared in (13), (27) and (29) are to be determined from the following set of equations.

$$a_{11}A_n + a_{12}B_n + a_{13}C_n + a_{14}D_n = 0 \tag{33}$$

$$a_{21}A_n + a_{22}B_n + a_{23}C_n + a_{24}D_n = 0 \tag{34}$$

$$a_{35}E_n + a_{36}F_n + a_{37}G_n + a_{38}H_n + a_{39}P_n + a_{310}Q_n = 0 \quad (35)$$

$$a_{45}E_n + a_{46}F_n + a_{47}G_n + a_{48}H_n + a_{49}P_n + a_{410}Q_n = 0 \quad (36)$$

$$a_{55}E_n + a_{56}F_n + a_{57}G_n + a_{58}H_n + a_{59}P_n + a_{510}Q_n = 0 \quad (37)$$

$$a_{65}E_n + a_{66}F_n + a_{67}G_n + a_{68}H_n + a_{69}P_n + a_{610}Q_n = 0 \quad (38)$$

$$a_{71}A_n + a_{72}B_n + a_{73}C_n + a_{74}D_n + a_{75}E_n + a_{76}F_n + a_{77}G_n + a_{78}H_n + a_{79}P_n + a_{710}Q_n = 0 \quad (39)$$

$$a_{81}A_n + a_{82}B_n + a_{83}C_n + a_{84}D_n + a_{85}E_n + a_{86}F_n + a_{87}G_n + a_{88}H_n + a_{89}P_n + a_{810}Q_n = 0 \quad (40)$$

$$a_{95}E_n + a_{96}F_n + a_{97}G_n + a_{98}H_n + a_{99}P_n + a_{910}Q_n + a_{911}S_{n1} + a_{912}S_{n2} = 0 \quad (41)$$

$$a_{105}E_n + a_{106}F_n + a_{107}G_n + a_{108}H_n + a_{109}P_n + a_{1010}Q_n + a_{1011}S_{n1} + a_{1012}S_{n2} = 0 \quad (42)$$

$$a_{11,1}A_n + a_{11,2}B_n + a_{11,3}C_n + a_{11,4}D_n + a_{11,5}E_n + a_{11,6}F_n + a_{11,7}G_n + a_{11,8}H_n + a_{11,9}P_n + a_{11,10}Q_n + a_{11,11}S_{n1} + a_{11,12}S_{n2} = b_{11} \quad (43)$$

$$a_{12,1}A_n + a_{12,2}B_n + a_{12,3}C_n + a_{12,4}D_n + a_{12,5}E_n + a_{12,6}F_n + a_{12,7}G_n + a_{12,8}H_n + a_{12,9}P_n + a_{12,10}Q_n + a_{12,11}S_{n1} + a_{12,12}S_{n2} = b_{12} \quad (44)$$

These equations are derived from the boundary and initial conditions (10), (22), (24), (25), (23), (26) and (11) respectively. All $a_{ij}'s$ are given in appendix. All the conditions and above equations are straightforward except equation (11) and corresponding to that (43) and (44). From (11) we see $u_{12} + p_1^{'} - p_2^{'} = P_2 - P_1 - \sigma_1(\pi_2 - \pi_1)$.

For even n, L.H.S. is zero and to make R.H.S. zero we are making some manipulation.

We are making $(P_2 - P_1) - \sigma_1(\pi_2 - \pi_1) = 45678.2859$ and as L.H.S. has $\cos\lambda_n x$, so by the Fourier series expansion we are arriving at the expression of b_{11} and b_{12} as follows $b_{11} = b_{12} = \{1-(-1)^n\}45678.2859$; where $p_1 = p_1^{'} + P_1$, $p_2 = p_2^{'} + P_2$

Using Gauss-Elimination method in which all the elements of the co-efficient matrix are complex has solved equations (33)--(44). In this computational tool we have introduced the complex arithmetic operations whenever it is required in the execution of the program.

3. Results and Discussion

In the above section we have generated the mathematical expression for various unknown variables. For the illustration of the above results a set of constants adopted here are as follows. $\mu_s = 0.00123$ kg/m sec., μ_R=0.00098 kg/m sec. (40% hematocrit) j=0.00000001121 m^2, γ=0.00000000000012 kg m/sec,

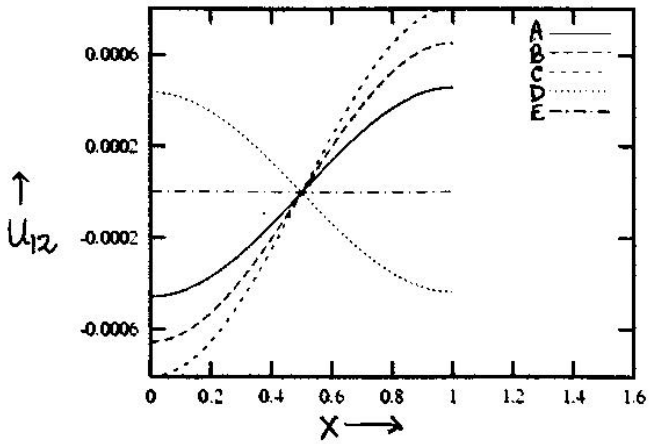

Fig.2 Vertical velocity distribution at the wall at different instants of time (A: $t = \pi/3$, B: $t = \pi/4$ C: $t = \pi/6$ D: $t = 3\pi/4$, E: $t = 3\pi/2$).

. $h = 0.0001$ m, L=0.02m. δ=0.00009m., S=0.1, $\alpha = 1.0$. Fig.2 is the representation of vertical velocity at the wall at different axial stations. Figure shows that fluid in the half of the considering length fluid is entering and in the left, it is departing from the tissue space. It is to be noted that the fluid movement from the channel space to the porous space is time dependent

From a careful investigation it is found that the vertical velocity can be made increase or decrease by changing various channel fluid parameters. As the primary objective of this investigation was how to control the fluid movement from channel to porous or vice-versa, one may use this model for several other studies. Here we have derived two non-dimensional constants $\frac{\rho L^2}{K_p \mu}$ and $\frac{\rho L}{\kappa \mu}$ as Tang and Fung [6]; but comparison with this said result has not been made because the construction of solution of the model differential equations in the present and foresaid studies are considerably different. Roughly, we observe that the configuration of graphs is as substantially similar to Tang and Fung [6] as expected.

To investigate the influential effect of rotational viscosity on the pressure distribution at the interface ($z = h$), we incorporate the Fig. 3. Here also, the appearance of each graph is resembled with the previous studies ([6], [11]). It can

be predicted that the decreasing values of μ_R increase the pressure at the interface. This may be for the rotation of blood cells enhances the fluid entrainment velocity into the tissue space. In the channel space the fluid particle get resistance for the presence of blood cells. Now, rotation of blood cell increase μ_R and consequently decrease the fluid pressure at the interface which fairly enrich the amount of fluid in the interstitial space. Therefore, the blood cell rotation has a significant impact on the interstitial fluid flow. The simple behavior of the axial velocity in the channel space appears in Fig.4. Profiles appear in this figures are quiet natural and obvious for the non-Newtonian fluid flow. As the wall is porous the axial velocity decreases along the vicinity of the wall. And along with that the no-slip condition of the axial velocity in the channel space at the wall is satisfied. The figure demonstrates the sharp time-dependency of the velocity and in some time-cycle it becomes negative. Apart from this, figure is also comparable with Misra and Ghosh [11] in which the solution representation and boundary conditions differ from the present situation. Again, near the wall the magnitude of the axial velocity is maximum which may be apprehended as the effect of micro-rotation.

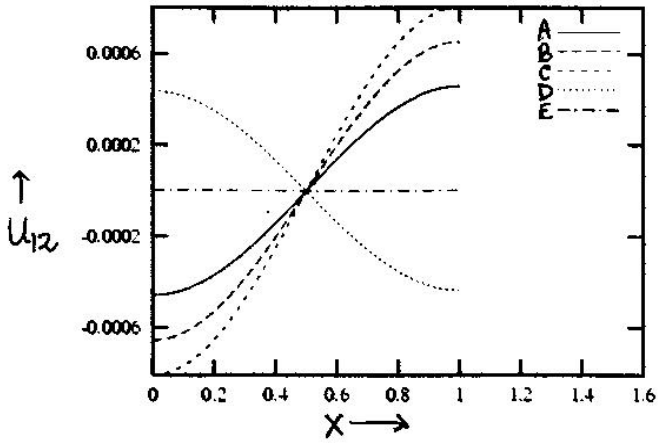

Fig.2 Vertical velocity distribution at the wall at different instants of time (A: $t = \pi/3$, B: $t = \pi/4$ C: $t = \pi/6$ D: $t = 3\pi/4$, E: $t = 3\pi/2$).

In the coupling flow, the study of wall shear stress is highly significant and that presented in the Figure 5 for various γ, the micro-rotational gradient coefficient. Here, Fig. 5 provides the idea of magnitude of wall shear stress at different axial stations. From fig. 5, it is observed that the increasing values of γ enhance the magnitude of wall shear stress.

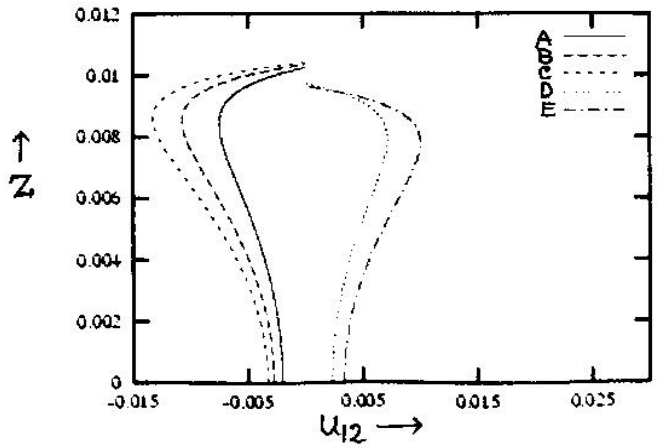

Fig.4 Axial velocity distribution in the channel space for some instants of time. (A: $t = \pi/3$, , B: $t = \pi/4$,C: $t = \pi/6$, D: $t = 3\pi/4$, E: $t = 3\pi/2$)

It follows that for the vertical velocity through the wall along with the parameter associated with rotational change with respect to vertical distance put forward an appreciable resistance on the flow in the channel along the axial direction. A brief numerical result on the interface vertical velocity and pressure distribution for different parameters first represented by Tang and Fung [6] are enclosed in the table. This shows that this parameter could be made responsible for various changes for the interstitial fluid movement.

From fig. 5, it is observed that the increasing values of γ enhance the magnitude of wall shear stress. It follows that for the vertical velocity through the wall along with the parameter associated with rotational change with respect to vertical distance put forward an appreciable resistance on the flow in the channel along the axial direction. A brief numerical result on the interface vertical velocity and pressure distribution for different parameters first represented by Tang and Fung [6] are enclosed in the table. This shows that this parameter could be made responsible for various changes for the interstitial fluid movement.

Vertical velocity and hydrostatic pressure in the porous matrix at the interface $z = h(t)$ for $\mu_s = 0.00123$ kg/m sec., μ_R =0.00098 kg/m sec.(40% hematocrit) j =0.00000001121 m^2, γ =0.00000000000012 kg m/sec, $h = 0.0001$ m, L=0.02m. δ =0.00009m., S=0.1, $\alpha = 1.0$, $\frac{\rho L^2}{K_p \mu} = 5 \times 10^Y$ and $\frac{\rho L}{\kappa \mu} = 5 \times 10^6$

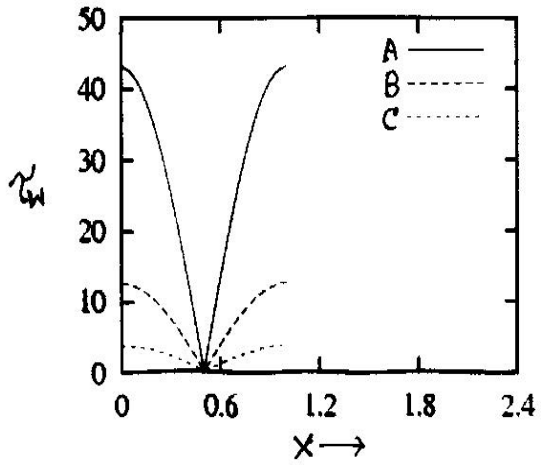

Fig.5 Wall shear stress distribution for various values of micro-rotational gradient coefficients (A: $\gamma = 12\times10^{-10}$, B: $\gamma = 12\times10^{-12}$, C: $\gamma = 12\times10^{-13}$).

x	Y	u_{12}	p_{12}
	6	2.765×10^{-4}	-9.911×10^{3}
	7	2.673×10^{-4}	-9.582×10^{3}
0.40	8	2.007×10^{-4}	-7.195×10^{3}
	9	5.798×10^{-5}	-2.061×10^{3}
	10	7.068×10^{-6}	-2.533×10^{2}
	6	-7.974×10^{-4}	2.858×10^{4}
	7	-7.710×10^{-4}	2.762×10^{4}
0.85	8	-5.789×10^{-4}	2.074×10^{4}
	9	-1.658×10^{-4}	5.942×10^{3}
	10	-0.382×10^{-5}	7.304×10^{2}

Acknowledgement: This research was financially supported by University Grant Commission under Minor Research Project scheme with Grant No. F. PSW-082/00-01 (ERO).

REFERENCES

1. C. Eringen and E. S. Suhubi, 1964 , 'Non-linear theory of simple micro-elastic solids-I', *Int. J. Engng Sci*., 2, 189—203
2. Grzegorz Lukaszewiez,1999, 'Micropolar Fluids Theory and Application', *BIRKHAUSER*,
3. A. Tozeren and R. Skalak, 1977, ' Micropolar fluids as models for suspensions of Rigid Sphere', *Int. J. Engng. Sci*., 15, 511-523
4. A. C. Eringen, 1966 'Theory of micropolar fluids' J. Math. Mech. Vol. 15, 1—16,
5. J. S. Lee and Y. C. Fung, 1970, 'Flow in a locally constricted tubes at low Reynolds number', *ASME, J. Appl. Mech*., 37, 9-16
6. H. T. Tang and Y. C. Fung,1975(a) ' Fluid movement in a channel with permeable walls covered by porous media- A model of lung alveolar sheet', *ASME, J. Appl. Mech.*42, 45—50
7. Y. C. Fung and H. T. Tang, 1975(b), 'Solute distribution in the flow in a channel bounded by porous layers---A model of the lung', *ASME, J. Appl. Mech.,* 42, 531-535
8. Y. C. Fung and H. T. Tang, 1975© ' Longitudinal Dispersion of tracer particles in the blood flowing in a pulmonary alveolar sheet', *ASME, J. Appl. Mech*. ,42, 136-140
9. T. Ariman,M. A. Truk and N. D. Sylvester, 1974, ' On steady and pulsatile flow of blood', *ASME, J. Appl. Mech.,* 41, 1-7
10. H. A. Hogan and M. Henriksen, 1989 , 'An evaluation of a micropolar model for Blood flow through a idealized stenosis' , *J. Biomechanics*, 22, 211—218
11. J. C. Misra and S. K. Ghosh, 1997 , ' A mathematical model for the study of blood flow through a channel with permeable wall', *Acta Mechanica*, 122, 137- 151
12. J. C. Misra and S. K. Ghosh , 2001, ' A mathematical model for the study of interstitial fluid movement vis-a -vis the non-Newtonian behavior of blood in a constricted artery', *Computers and Mathematics,* 41, 783---811